# Turbulent Boundary Layer Control based on DBD Plasma-Actuator-Generated Vortices

## C.W. Wong, X.Q. Cheng, Y.C. Liu and Y. Zhou

Shenzhen Digital Engineering Laboratory of Offshore Equipment, Institute of Turbulence-Noise-Vibration Interactions and Control, Shenzhen Graduate School, Harbin Institute of Technology, Shenzhen, 518055, China

## Abstract

This paper presents the experimental investigation on the drag change of a turbulent boundary layer using dielectric barrier discharge DBD plasma actuators. Five streamwise-oriented plasma actuator configurations were designed to generate counter-rotating vortices of different sizes based on various actuator lengths. While the time-resolved PIV was used to capture the development of the streamwise vortices in a plane normal to the mean flow, a hotwire anemometry was used to measure the spanwise distribution of drag change under manipulation. It has been found that the longest plasma actuator may maximize the local drag reduction and the spanwise region of drag reduction behind an actuator pair. Further, the spanwise drag change behind an actuator pair is largely affected by the wall jet velocity and streamwise vorticity. We believe that both the wall jet velocity and the streamwise vorticity should not be too high in order to achieve drag reduction.

## Introduction

Drag reduction in turbulent boundary layers (TBL) has received widespread attention in literature and its potential benefits in various engineering applications cannot be overlooked. The understanding of turbulence generation mechanism is crucial for developing methods for the control of TBL with a view to reduce skin-friction drag. It has been widely recognized that vortices cause the velocity streaks by advecting the mean velocity gradient (e.g. Blackwelder & Eckelmann 1979 [1]), therefore leading to the creation of new vortical structures near wall. One approach is to suppress vortex regeneration based on the stabilizing or weakening the basic flow streaks (Jimenez & Pinelli 1999 [2]). The study by Schoppa & Hussain (1998) [3] gives crucial support for stabilizing streaks based on large-scale streamwise vortices in a turbulent channel flow. Evidently, the large-scale streamwise vortices are one of the most promising techniques to manipulate the stability, spacing, and strength of near-wall low-speed streaks, and hence achieving drag reduction (e.g. Di Cicca et al. 2002 [4]; Iuso et al. 2002 [5]).

The application of DBD plasma actuator is rather extensively used in laminar and turbulent flow separation control on streamlined and bluff bodies. To our best knowledge, successful drag reduction in a turbulent boundary layer based on DBD plasma actuators is rather scarce. Choi et al. (2011) [6] studied two configurations of DBD plasma actuators for the control of a turbulent boundary layer over a flat plate. Their DBD plasma actuators were aligned in the streamwise direction to produce forcing along the spanwise direction. Both spanwise oscillation and spanwise travelling waves could be produced, depending on the direction of the induced flow of each actuator. Their manipulation modified the near-wall flow structures. Based on their previous experimental findings associated with other flow control devices (e.g. Choi et al. 1998 [7]; Choi & Clayton 2001

[8]), they suggested that the plasma-actuator-generated spanwise oscillation and travelling waves could lead to a drag reduction of 45%, though the drag change was not measured in their investigation. Li et al. (2014) [9] and Wong et al. (2015) [10] investigated experimentally the plasma-actuator-generated vortices for the control of a turbulent boundary layer over a flat plate, and managed an average skin-friction drag reduction up to 20%. The plasma-actuator-generated vortices made a pronounced effect on the flow structures all the way up to $y^+ \leq 100$. When the plasma was introduced, the reorganized TBL showed an increased energy dissipation rate in the near wall region that contributed to drag reduction. The upwash of plasma-generated counter-rotating vortex pair pumped the low-momentum fluid away from the wall, leading to a region of lower-speed and stabilized fluid near wall.

In spite of extensive investigations on turbulent boundary-layer control, many aspects of skin-friction drag reduction based on plasma actuators have yet to be clarified. For example, how do the plasma-actuator-generated vortices of different sizes influence the local drag change? The first objective of this work is to investigate experimentally the five DBD plasma-actuator configurations for the generation of streamwise vortices of different sizes (these vortices have the same streamwise vorticity at the trailing edge of actuator), and their development in the turbulent boundary layer. The second objective of this work is to examine drag change under the manipulation based on DBD plasma actuators.

## Experimental Details

Experiments were performed in a closed-loop wind tunnel, with a test section of $L \times W \times H = 5.5 \times 0.8 \times 1.0$ m. A rounded leading-edge flat plate with $L \times W \times H = 4.8 \times 0.78 \times 0.015$ m was installed vertically in the test section, and an adjustable end plate was set at an angle of 12° to avoid the leading-edge flow separation. Two rows of screws were installed at $x = 100$ mm downstream of the leading-edge of the flat plate to generate fully developed turbulent boundary-layer at the measurement station ($x = 3.2$ m) in the free-stream velocity $U_\infty$ of 2.4 m/s. The boundary layer thickness $\delta$ was 85 mm at the measurement station, while the Reynolds number $Re_\theta = 1100$ based on the momentum thickness $\theta$, and the wall unit length $l = 150$ μm without perturbation.

The DBD plasma actuator consisted of two copper electrodes separated by a dielectric panel made of PMMA. The actuator was flush-mounted to the wall surface, and the protrusion of the upper electrode from the wall was negligible. Plasma was generated by applying a sinusoidal AC waveform to the upper electrodes with voltage $V_a = 9.0 - 15.0$ kV$_{p-p}$ at frequencies $f = 2$ kHz, with the lower electrodes connected to ground. The length $L$ of the streamwise-orientated DBD plasma actuator is defined as the distance between the leading edge and the trailing edge of the

discharged region. Five plasma actuators, each with different $L$ (20, 40, 60, 80 and 100 mm), have been investigated. The vortex size was controlled by $L$, and the maximum streamwise vorticity of all actuator configurations was kept at an approximately constant value (200 s$^{-1}$) through tuning the $V_a$. Note that the spacing $D$ between an actuator pair was determined by the size of the vortices generated by the actuator. The selection of $D$ is important because all actuator configurations generate streamwise counter-rotating vortex pair, and the vortices do not collide with each other along the entire electrode length. The sketch of the overall configuration is shown in Fig. 1.
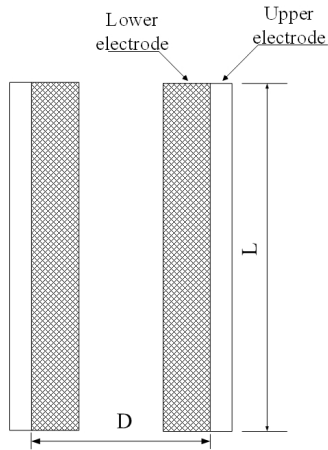


Figure 1. Schematic of a DBD plasma actuator configuration.

A miniature single wire probe (55P11) operated at an overheat ratio of 1.8 on a constant-temperature anemometer (Dantec Streamline CTA) was used to measure the streamwise velocity fluctuation $u$ in the boundary layer. The sensing element was a tungsten wire of 5 μm diameter and about 1 mm length, and was calibrated in the freestream flow using the Pitot static tube. The hot-wire probe was mounted on a sting supported by a computer-controlled three-dimensional (3D) traversing mechanism, whose resolution in the $y$ direction was 10 μm. The hotwire signals were offset, amplified, low-pass filtered with a cut-off frequency of 1.0 kHz, and digitized using the 16-bit analogue-to-digital A/D board at a sampling frequency of 3 kHz. The sampling duration for each measurement point was 40s, and therefore ensuring the convergence of the root-mean-square of $u$ and giving an uncertainty of no more than ±1%.
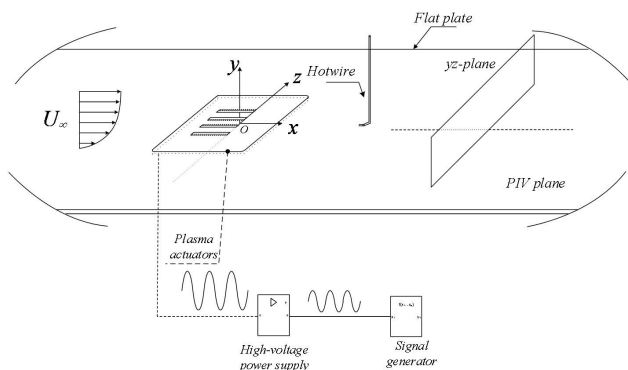


Figure 2. Schematic of overall experimental setup.

A LaVision PIV system was used to measure the turbulent boundary layer in two $y$-$z$ planes with plasma control. Both the laser (a maximum energy output of 30 mJ per pulse) and the camera were mounted to the side of the wind tunnel, and the streamwise location of the laser sheet (1.2 mm thick) was

precisely controlled by the 3D traversing mechanism. The CCD camera (double frames, 2016 pixels × 2016 pixels) viewed the $y$-$z$ plane via a 0.94 $\delta$ × 1.41 $\delta$ (80 × 150 mm) optical mirror placed at $x$ = 510 mm (3400$l$), 45° with respect to the $y$-$z$ plane. The flow interference due to the presence of the mirror was considered to be negligible because the velocity vectors of $y$- and $z$-direction over the plane were less than 2% of $U_\infty$ for uncontrolled case. Images were taken with a 180 mm f/2.8 lens while the aperture was set fully open. The flow field captured by the camera was 150 mm × 150 mm (1000$l$ × 1000$l$), while an image area of $z^+$ = -500 to +150 and $y^+$ = -100 to +400 was carefully examined. Image pairs were taken at 300 Hz, with the time delay between frames being 150 μs to allow image capturing with more valid particles. The flow was seeded with peanut oil particles with an average 1 μm in diameter generated by a TSI 9307-6 particle generator. A total of 400 image pairs were obtained for each plane. In the image processing, spatial cross-correlation algorithm over 32 × 32 interrogation area with 50% overlap to determine the velocity and vorticity vector fields. The uncertainty of the mean velocity and the vorticity was no more than ±1%. The schematic of overall experimental setup is shown in Fig. 2.

**Results and Discussions**
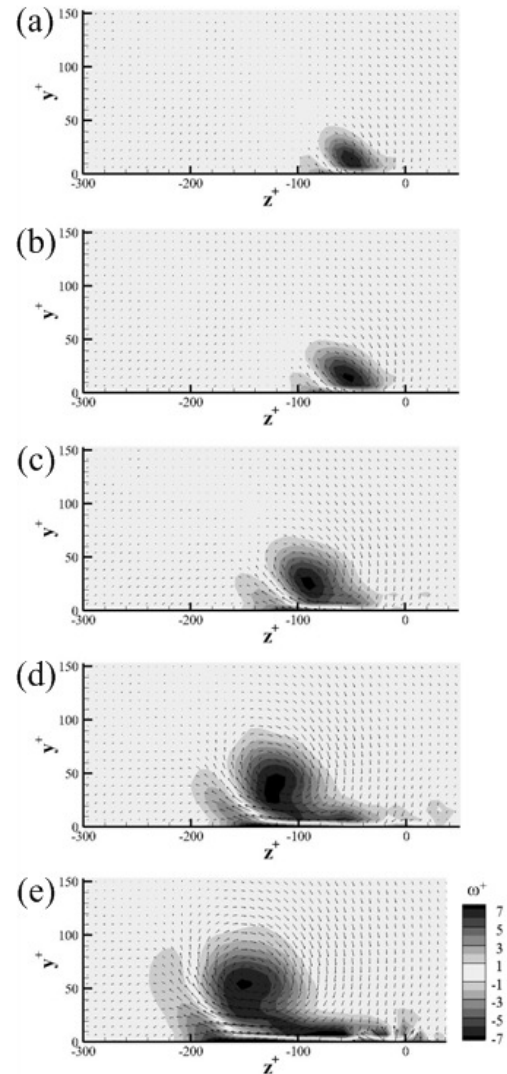


Figure 3. Plasma-actuator-generated vortices of different sizes (measured at the trailing edge of the actuator). (a) $L$ = 20; (b) $L$ = 40; (c) $L$ = 60; (d) $L$ = 80; (e) $L$ = 100 mm.

At a constant $V_a$, the ionic wind velocity generated by the DBD plasma actuator in quiescent air would be approximately a constant irrespective of the change in $L$. The longest actuator would generate the largest vortex since the plasma imparts the greatest momentum into the flow. However, the increased $L$ leads to the reduction of the maximum streamwise vorticity in the turbulent boundary layer.

In order to generate different vortex size while maintaining an approximately constant streamwise vorticity, five DBD plasma actuators, each with different $L$ (20, 40, 60, 80 and 100 mm), have been considered. Figure 3 shows the plasma-generated streamwise vortices in the $y$-$z$ plane, captured at the trailing edge of a single plasma actuator. It can be seen that an approximately constant maximum streamwise vorticity of 200 s$^{-1}$ is achieved in all actuator configurations due to fact that the $V_a$ is increased from 9 to 13 kV$_{p-p}$. In fact, a suitable $V_a$ is searched for each actuator configuration; the actuator with an $L$ of 20, 40, 60, 80 and 100 correspond to 9, 10, 11, 12 and 13 kV$_{p-p}$, respectively. Fig. 3 also shows that the lateral location of the vortex core increases with increasing electrode length due to the longer contact time with the DBD. Based on the PIV data achieved in Fig. 3, $D$ is considered to be twice of the spanwise distance which covers both the primary and the secondary vortices generated by a single actuator. For examples, the $D$ for an actuator pair with an $L$ of 20, 60 and 100 correspond to 32, 60 and 80 mm, respectively.
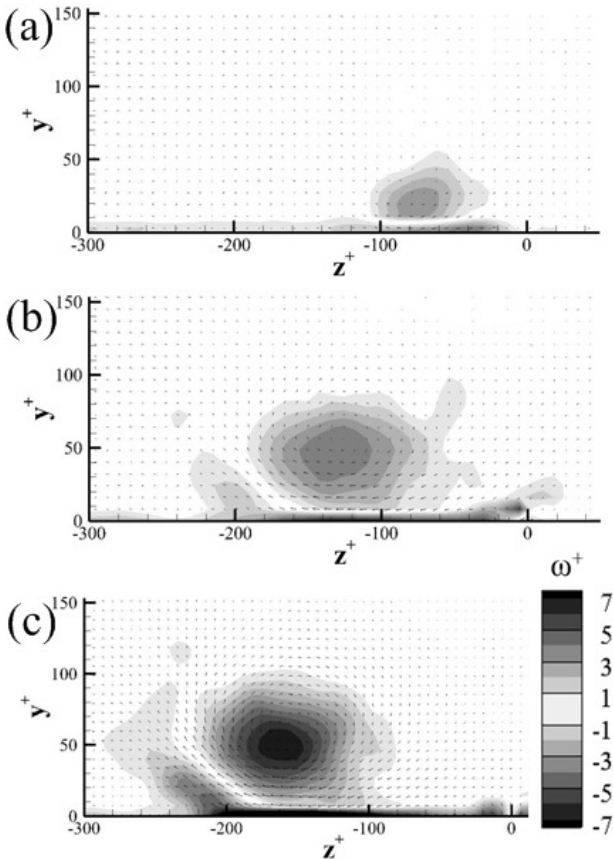


Figure 4. Plasma-actuator-generated vortices of different sizes (measured at 25 mm downstream the trailing edge of the actuator). (a) $L = 20$; (b) $L = 60$; (c) $L = 100$ mm.

The plasma-actuator-generated flow-field at a distance of 25 mm downstream from the trailing edge of the actuator is shown in Fig. 4. At a fixed electrode length, the streamwise vorticity is reduced

due to the loss of wall jet velocity to the skin friction near wall. Here, we believe that each DBD plasma actuator produces a wall jet in the spanwise direction that feeds into the streamwise vorticity from below to increase its vorticity. It is noteworthy that the wall jet produced by the shortest actuator is smaller than that by the longer actuator; therefore, the maximum streamwise vorticity generated by the longest actuator is higher than that generated by the shortest actuator. The size of vortex increases radially (Fig. 4) when one compares the data achieved at the trailing edge of the actuator (Fig. 3). As a result, the lateral location of the vortex core is moved away from the origin of discharge (Fig. 4). It should be noted that the vortex size is about 100 and 50 wall units for the longest and shortest actuator configurations, respectively.
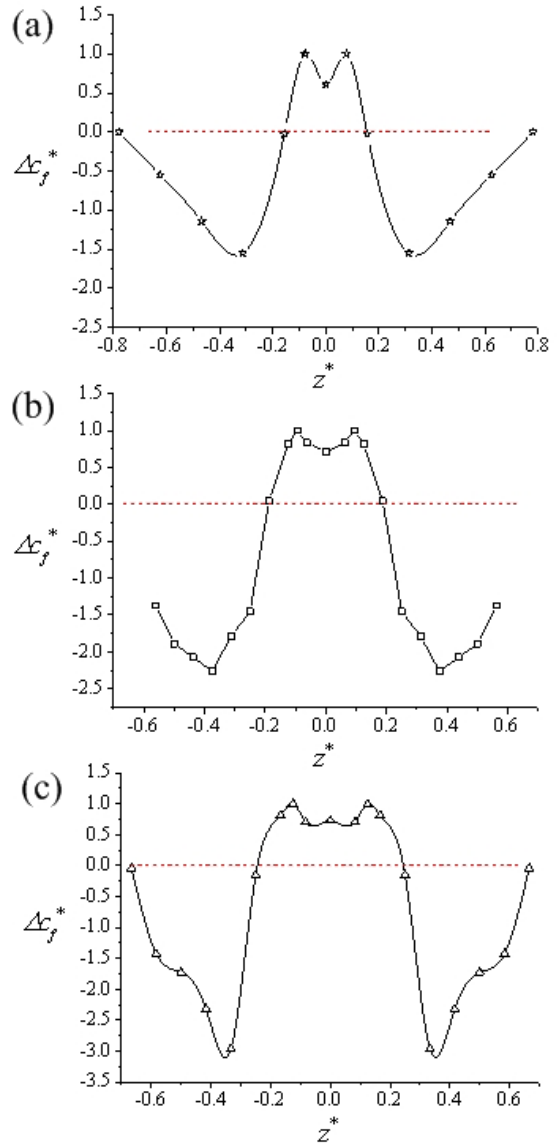


Figure 5. Spanwise distribution of drag change at 25 mm behind one pair of actuator. (a) $L = 20$; (b) $L = 60$; (c) $L = 100$ mm.

Figure 5 shows the spanwise distribution of drag change $\Delta C_f^*$ $(= \overline{(\tau_w)}_{off} - \overline{(\tau_w)}_{on} / \overline{(\tau_w)}_{off} \times 100\%)$ at 25 mm behind one pair of actuator, where $\overline{\tau_w} = \mu(\partial \overline{U}/\partial y)_{|y=0}$. The $\overline{(\tau_w)}_{on}$ and $\overline{(\tau_w)}_{off}$ are the wall shear stress in the viscous sublayer with and without plasma actuation, respectively. Note that the $\partial \overline{U}/\partial y$ near wall was

estimated by linear fitting of five measurement points within the viscous sublayer. The spacing between two consecutive measurement points was 50 μm (0.33$l$). The maximum local drag reduction is 21.9%, 26.7% and 37.9% for the actuator with $L$ of 20, 60 and 100 mm, respectively. It is certain that large vortices generated by the longest actuator leads to the highest local drag reduction compared with other actuators because the large streamwise vorticity allows the removal of low momentum fluid near wall. However, there exists a large region of drag increase when one considers the spanwise distribution of drag change behind an actuator. This is due to the fact that the wall jet velocity by the longest plasma actuator is the highest among all actuators, and the plasma-actuator-generated vortices do not lift up above the wall. As a result, the large near-wall jet velocity and a relatively strong downwash enhance the drag increase. We believe that the longest actuator, i.e. the largest vortex size, should be used for the purpose of drag reduction due to the fact that a large region of drag reduction exists between the vortex pair. In addition, a relatively weak streamwise vorticity, i.e. a reduced wall jet velocity, should be deployed in order to minimize the drag increase regions exist on either sides of an actuator pair.

## Conclusions

Control of turbulent boundary using DBD plasma-actuator-generated vortices has been performed. Following conclusions can be drawn:

(1) The size of the vortex can be controlled by the length of the actuator, while the streamwise vorticity can be adjusted by changing the applied voltage. Five actuators were investigated, they produce an approximately the same streamwise vorticity, but different vortex size. The longest and the shortest actuator produce the largest and the smallest vortex, respectively.

(2) Large vortices generated by the longest actuator leads to the highest local drag reduction compared with other actuators. However, there exists a large region of drag increase when one considers the spanwise drag distribution behind the actuator. Here, we propose that a longer actuator, i.e. $L > 100$ mm, that generates large vortex pairs with relatively weak vorticity should be used in order to achieve considerable drag reduction in a turbulent boundary layer.

## Acknowledgments

## References

[1] Blackwelder, R. & Eckelmann, H., Streamwise Vortices Associated with the Bursting Phenomenon, *J. Fluid Mech.*, **94**, 1979, 577-594.

[2] Jimenez, J. & Pinelli, A., The Autonomous Cycle of Near-Wall Turbulence, *J. Fluid Mech.*, **389**, 1999, 335-359.

[3] Schoppa, W. & Hussain, F., A Large-Scale Control Strategy for Drag Reduction in Turbulent Boundary Layers, *Phys. Fluids*, **10**, 1998, 1049-1051.

[4] Di Cicca, G., Iuso, G., Spazzini, P. & Onorato, M., PIV Study of the Influence of Large-Scale Streamwise Vortices on a Turbulent Boundary Layer, *Exp. Fluids*, **33**, 2002, 663-669.

[5] Iuso, G., Onorato, M., Spazzini, P. G. & Di Cicca, G. M., Wall Turbulence Manipulation by Large-Scale Streamwise Vortices, *J. Fluid Mech.*, **473**, 2002, 23-58.

[6] Choi, K.-S., Jukes, T. & Whalley, R., Turbulent Boundary-Layer Control with Plasma Actuators, *Phil. Trans. R. Soc. A*, **369**, 2011, 1443-1458.

[7] Choi, K.-S., DeBisschop, J.-R. & Clayton, B.R., Turbulent Boundary-Layer Control by means of Spanwise-Wall Oscillation, *AIAA J.*, **36**, 1998, 1157-1163.

[8] Choi, K.-S. & Clayton, B. R., The Mechanism of Turbulent Drag Reduction with Wall Oscillation, *Intl J. Heat Fluid Flow*, **22**, 2001, 1-9.

[9] Li, Y.P., Wong, C.W., Li, Y.Z., Zhang, B.F. & Zhou, Y., Drag Reduction of a Turbulent Boundary Layer Using Plasma Actuators, 19th Australasian Fluid Mechanics Conference, 8-11 December 2014, Melbourne, Australia, Paper 340.

[10] Wong, C.W., Cheng, X.Q., Li, Y.Z. & Zhou, Y., Active Drag Reduction in a Turbulent Boundary Layer Using Plasma Actuators, Proceedings of the FLUCOME2015, November 15-18, 2015, Doha, Qatar, Paper 011.